J|A|C|S
ARTICLES

Published on Web 08/14/2009

High Oxidation State Rhodium and Iridium Bis(silyl)dihydride Complexes Supported by a Chelating Pyridyl-Pyrrolide Ligand

Jennifer L. McBee, Jose Escalada, and T. Don Tilley*

Department of Chemistry, University of California, Berkeley, Berkeley, California 94720

Received April 30, 2009; E-mail: tdtilley@berkeley.edu

Abstract: New rhodium and iridium complexes containing the bidentate ligand 3,5-diphenyl-2-(2-pyridyl)pyrrolide (PyPyr) were prepared. The bis(ethylene) complex (PyPyr)Rh(C_2H_4)$_2$ (**3**) reacted with $HSiEt_3$, $HSiPh_3$, and HSi^tBuPh_2 to produce the 16-electron Rh(V) bis(silyl)dihydrides (PyPyr)Rh(H)$_2$($SiEt_3$)$_2$ (**8**), (PyPyr)Rh(H)$_2$($SiPh_3$)$_2$ (**9**), and (PyPyr)Rh(H)$_2$(Si^tBuPh_2)$_2$ (**10**), respectively. The analogous Ir(V) bis(silyl)dihyride (PyPyr)Ir(H)$_2$($SiPh_3$)$_2$ (**11**) has also been synthesized. X-ray crystallography reveals that **9**−**11** adopt a coordination geometry best described as a bicapped tetrahedron. Silane elimination from **9** and **10** occurred in the presence of either $HSiEt_3$ or PPh_3. Mechanistic studies of the silane exchange process involving **10** and free $HSiEt_3$ (to give **8**) indicate that this process occurs by rate-limiting reductive elimination of HSi^tBuPh_2 from **10** to generate a 14-electron Rh(III) intermediate of the type (PyPyr)Rh(H)(Si^tBuPh_2).

Introduction

The activation of Si−H bonds by late transition metal complexes represents an important step in numerous catalytic reactions,[1−10] including silane redistribution,[11−15] reductions of haloarenes by silanes,[16−18] and the dehydrogenative Si−C coupling of silanes with arenes.[3,19−24] Complexes of Rh and Ir feature prominently in known Si−H bond activation chemistry, and this may be at least partly due to the ability of metals to support silyl complexes in high oxidation states.[25−36] In addition, these metals may activate Si−H bonds by way of formation of η^2-silane complexes.[37−41] Thus, it is of interest to explore new Si−H bond activations and related catalytic transformations for group 9 metal complexes, and in this context it is worth noting that most of the previous investigations have featured soft ancillary donor ligands (e.g., cyclopentadienyl and phosphine derivatives). Fewer investigations have involved silane conver-

(1) Corey, J. Y.; Braddock-Wilking, J. *Chem. Rev.* **1999**, *99*, 175–292.
(2) Tilley, T. D. In *The Chemistry of Organic Silicon Compounds*; Patai, S., Rappoport, Z., Eds.; Wiley: New York, 1989.
(3) Tilley, T. D. *Comments Inorg. Chem.* **1990**, *10*, 37–46.
(4) Tilley, T. D. In *The Silicon-Heteroatom Bond*; Patai, S., Rappoport, Z., Eds.; Wiley: New York, 1991.
(5) *Catalyzed Direct Reactions of Silicon*; Lewis, K. M.; Rethwisch, D. G., Eds.; Elsevier: Amsterdam, The Netherlands, 1993.
(6) Waterman, R.; Hayes, P. G.; Tilley, T. D. *Acc. Chem. Res.* **2007**, *40*, 712–719.
(7) Eisen, M. S. In *The Chemistry of Organosilicon Compounds*; Rappoport, Z., Apeloig, Y., Eds.; Wiley: New York, 1998.
(8) *Comprehensive Handbook of Hydrosilation*; Marciniec, B., Gulinski, J., Urbaniak, W., Kornetka, Z. W., Eds.; Pergamon: Oxford, 1992.
(9) Ong, C. M.; Burchell, T. J.; Puddephatt, R. J. *Organometallics* **2004**, *23*, 1493–1495.
(10) Bosnich, B. *Acc. Chem. Res.* **1998**, *31*, 667–674.
(11) Gavenonis, J.; Tilley, T. D. *Organometallics* **2004**, *23*, 31–43.
(12) Hashimoto, H.; Tobita, H.; Ogino, H. *J. Organomet. Chem.* **1995**, *499*, 205–211.
(13) Radu, N. S.; Hollander, F. J.; Tilley, T. D. *Chem. Comm.* **1996**, *21*, 2459–2460.
(14) Curtis, M. D.; Epstein, P. S. *Adv. Organomet. Chem.* **1981**, *19*, 213–232.
(15) Sharma, H. K.; Pannell, K. H. *Chem. Rev.* **1995**, *95*, 1351–1374.
(16) Alonso, F.; Beletskaya, I. P.; Yus, M. *Chem. Rev.* **2002**, *102*, 4009–4092.
(17) Boukherroub, R.; Chatgiliaoglu, C.; Manuel, G. *Organometallics* **1996**, *15*, 1508–1510.
(18) Esteruelas, M. A.; Herrero, J.; Lopez, F. M.; Martin, M.; Oro, L. A. *Organometallics* **1999**, *18*, 1110–1112.
(19) Corey, J. Y. *Adv. Organomet. Chem.* **2004**, *51*, 1–52.
(20) Gauvin, F.; Harrod, J. F.; Woo, H. G. *Adv. Organomet. Chem.* **1988**, *42*, 363–405.
(21) Ezbiansky, K.; Djurovich, P. I.; LaForest, M.; Sinning, D.; Zayes, R.; Berry, D. H. *Organometallics* **1998**, *17*, 1455–1457.
(22) Tsukada, N.; Hartwig, J. F. *J. Am. Chem. Soc.* **2005**, *127*, 5022–5023.
(23) Murata, M.; Ishikura, M.; Nagata, M.; Watanabe, S.; Masuda, Y. *Org. Lett.* **2002**, *4*, 1843–1845.
(24) Manoso, A. S.; DeShong, P. *J. Org. Chem.* **2001**, *66*, 7449–7455.
(25) Cook, K. S.; Incarvito, C. D.; Webster, C. E.; Fan, Y. B.; Hall, M. B.; Hartwig, J. F. *Angew. Chem., Int. Ed.* **2004**, *43*, 5474–5477.
(26) Duckett, S. B.; Haddleton, D. M.; Jackson, S. A.; Perutz, R. N.; Poliakoff, M.; Upmacis, R. K. *Organometallics* **1988**, *7*, 1526–1532.
(27) Duckett, S. B.; Perutz, R. N. *Chem. Comm.* **1991**, *1*, 28–31.
(28) Fernandez, M. J.; Bailey, P. M.; Bentz, P. O.; Ricci, J. S.; Koetzle, T. F.; Maitlis, P. M. *J. Am. Chem. Soc.* **1984**, *106*, 5458–5463.
(29) Fernandez, M. J.; Maitlis, P. M. *Dalton Trans.* **1984**, *9*, 2063–2066.
(30) Feldman, J. D.; Peters, J. C.; Tilley, T. D. *Organometallics* **2002**, *21*, 4065–4075.
(31) Fernandez, M. J.; Maitlis, P. M. *Organometallics* **1983**, *2*, 164–165.
(32) Gutierrez-Puebla, E.; Monge, A.; Paneque, M.; Poveda, M. L.; Taboada, S.; Trujillo, M.; Carmona, E. *J. Am. Chem. Soc.* **1999**, *121*, 346–354.
(33) Klei, S. R.; Tilley, T. D.; Bergman, R. G. *Organometallics* **2002**, *21*, 4648–4661.
(34) Loza, M. L.; de Gala, S. R.; Crabtree, R. H. *Inorg. Chem.* **1994**, *33*, 5073–5078.
(35) Tanke, R. S.; Crabtree, R. H. *Organometallics* **1991**, *10*, 415–418.
(36) Turculet, L.; Feldman, J. D.; Tilley, T. D. *Organometallics* **2004**, *23*, 2488–2502.
(37) Bart, S. C.; Lobkovsky, E.; Chirik, P. J. *J. Am. Chem. Soc.* **2004**, *126*, 13794–13807.
(38) Delpech, F.; Sabo-Etienne, S.; Chaudret, B.; Daran, J. C. *J. Am. Chem. Soc.* **1997**, *119*, 3167–3168.
(39) Lin, Z. *Chem. Soc. Rev.* **2002**, *31*, 239–245.
(40) Schneider, J. J. *Angew. Chem., Int. Ed.* **1996**, *35*, 1068–1075.
(41) Taw, F. L.; Bergman, R. G.; Brookhart, M. *Organometallics* **2004**, *23*, 886–890.

Scheme 1

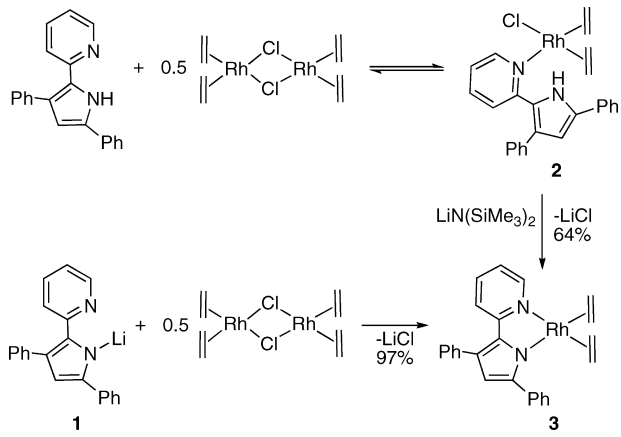

sions at group 9 metal centers supported by hard ancillary ligands with oxygen or nitrogen donos.[42]

Recent investigations in these laboratories have explored use of the monoanionic, chelating 2-(2-pyridyl)indolide (PyInd) ligand with late transition metals.[42,43] Interestingly, this ligand stabilizes coordinatively unsaturated Ir(V) and Rh(V) bis(silyl)dihydride complexes. The solid-state structure of the Ir(V) complex, (PyInd)Ir(H)$_2$(SiPh$_2$Me)$_2$, revealed a highly distorted octahedral geometry. Furthermore, the Rh(V) bis(silyl)dihydride (PyInd)Rh(H)$_2$(SiEt$_3$)$_2$ mediates the catalytic dehydrochlorinative coupling of chlorobenzene with triethylsilane.

Given the results observed for (PyInd)Rh and (PyInd)Ir complexes, it was of interest to examine related systems with nitrogen-donor ligands that possess different steric and/or electronic properties. In this regard, the ligand 3,5-diphenyl-2-(2-pyridyl)pyrrolide (PyPyr), reported by McNeill and coworkers,[44] seemed of interest as it is more sterically demanding than PyInd. The PyPyr ligand has been found to support late-metal complexes in relatively high oxidation states, such as (PyPyr)AuMe$_2$[45] and (PyPyr)PtMe$_3$.[46]

This report describes the synthesis, structure and reactivity of Rh and Ir complexes containing the PyPyr ligand. This ligand, like PyInd, supports Rh(V) and Ir(V) bis(silyl)dihydrides which also exhibit geometries that are highly distorted from an ideal octahedron. Interestingly, the rhodium complexes have been found to exchange silyl hydride ligands with added tertiary silanes, and these reactions appear to proceed via 14 electron (PyPyr)Rh(H)(SiR$_3$) intermediates.

Results and Discussion

Synthesis of (PyPyr)M(alkene)$_2$ Complexes. The Rh(I) complexes were prepared using both (PyPyr)H and Li(PyPyr) (**1**) as reagents (Scheme 1). Treatment of (PyPyr)H with LiN(SiMe$_3$)$_2$ or ^{n}BuLi in benzene afforded Li(PyPyr) (**1**) as a yellow powder in good yields (75−91%) after removal of solvent in vacuo. Excess LiN(SiMe$_3$)$_2$ or ^{n}BuLi was removed by washing the isolated solid with hexane. The ^{1}H NMR spectrum of **1** in benzene-d_6 contains only broad aromatic peaks and confirms the complete consumption of starting material. In subsequent procedures, this solid was used without further purification.

Scheme 2

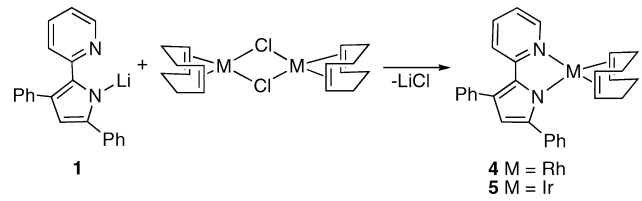

Addition of (PyPyr)H to 0.5 equiv of [RhCl(C$_2$H$_4$)$_2$]$_2$[47] in toluene proceeded partially (in 52% yield) to (PyPyrH)RhCl(C$_2$H$_4$)$_2$ (**2**), characterized by ^{1}H NMR spectroscopy as part of an equilibrium mixture with (PyPyr)H and [RhCl(C$_2$H$_4$)$_2$]$_2$ (Scheme 1). Subsequent treatment of this mixture with LiN(SiMe$_3$)$_2$ in benzene generated (PyPyr)Rh(C$_2$H$_4$)$_2$ (**3**), which was isolated in 64% yield. A more direct route to **3** was accomplished via addition of **1** to [RhCl(C$_2$H$_4$)$_2$]$_2$ in benzene. After filtration and removal of the solvent in vacuo, complex **3** was isolated in 97% yield as an analytically pure solid.

At 25 °C, the ^{1}H NMR spectrum of **3** in benzene-d_6 exhibits three broad vinylic resonances at 2.06 (2H), 2.86 (2H), and 3.07 (4H) ppm associated with the two ethylene ligands. Investigation of the ^{1}H NMR spectrum of **3** by low temperature ^{1}H NMR spectroscopy revealed that the ethylene resonance at 3.07 ppm decoalesces into two resonances at 4.08 (2H) and 2.09 (2H) ppm at −60 °C. The assignments of the ^{1}H NMR resonances of the ethylene ligands in **3** are based on 1D NOESY at −60 °C. The ^{1}H NMR resonance at 3.07 ppm corresponds to the four protons of the ethylene ligand *cis* to the pyrrolide donor and *trans* to the pyridyl ligand donor. The free energy of activation for the rotation of this ethylene ligand was determined to be 9.1 ± 2 kcal/mol at −60 °C.

The Rh(I) and Ir(I) complexes with 1,5-cyclooctadiene (COD) as the ancillary ligand were obtained by a method similar to that used for **3**, via a salt metathesis reaction (Scheme 2). Addition of a slurry of **1** in benzene to a solution of [(COD)RhCl]$_2$[48] in benzene gave the brown solid (PyPyr)Rh(COD) (**4**) in 51% yield after recrystallization by vapor diffusion of pentane into a benzene solution of **4** at 25 °C. The Ir analogue was synthesized in a similar manner, from **1** and [(COD)IrCl]$_2$,[49] to give analytically pure orange platelets of (PyPyr)Ir(COD) (**5**) in 34%. The ^{1}H NMR spectrum of **4** in benzene-d_6 is similar to that of **3** in that the COD ligand occupies two inequivalent coordination sites, as indicated by two vinylic resonances (3.63 and 4.63 ppm) in the ^{1}H NMR spectrum. Similarly for **5**, two vinylic proton resonances for the COD ligand are observed at 3.39 and 4.60 ppm.

Compounds **4** and **5** crystallized with isostructural solid-state structures in the space group *C*2/*c* (Figures 1 and 2). The pyridyl and pyrrolide ligand fragments are coplanar, while the phenyl substituents twist out of the pyrrolide plane. This aspect of the molecular structure may be described by the torsion angles between the phenyl planes and the pyridyl plane, which are 74° and 46° for **4** and 74° and 47° for **5**. These structures are similar to that previously observed for [(bipy)Rh(COD)]PF$_6$,[50] as indicated by comparison of N−M−N angles (ca. 79°) and N−M bond distances (∼2.09 Å, Table 1).

(42) Karshtedt, D.; Bell, A. T.; Tilley, T. D. *Organometallics* **2006**, *25*, 4471–4482.
(43) Karshtedt, D.; McBee, J. L.; Bell, A. T.; Tilley, T. D. *Organometallics* **2006**, *25*, 1801–1811.
(44) Klappa, J. J.; Rich, A. E.; McNeill, K. *Org. Lett.* **2002**, *4*, 435–437.
(45) Schouteeten, S.; Allen, O. R.; Haley, A. D.; Ong, G. L.; Jones, G. D.; Vicic, D. A. *J. Organomet. Chem.* **2006**, *691*, 4975–4981.
(46) Luedtke, A. T.; Goldberg, K. I. *Inorg. Chem.* **2007**, *46*, 8496–8498.
(47) Cramer, R. *Inorg. Syn.* **1990**, *28*, 86.
(48) Giordano, G.; Crabtree, R. H. *Inorg. Syn.* **1990**, *28*, 88.
(49) Herde, J. L.; Lambert, J. C.; Senoff, C. V. *Inorg. Syn.* **1974**, *15*, 18.
(50) Alejandro, F.; Guadalupe, A. R.; Huang, S. D. *Z. Kristallogr-New Crystal Structures* **1999**, *214*, 463.

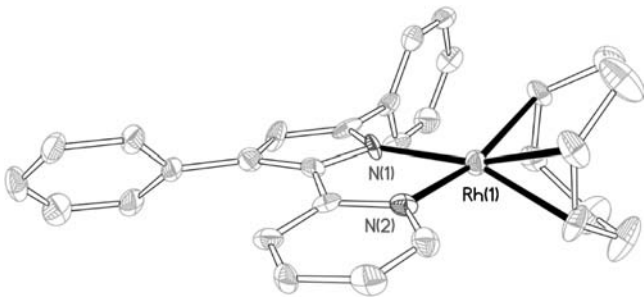

Figure 1. ORTEP diagram of the X-ray crystal structure of **4**. Hydrogen atoms are omitted for clarity. Bond lengths (Å) and angles (deg): Rh1−N1 = 2.079(7), Rh1−N2 = 2.094(7), ∠N1−Rh1−N2 = 79.1(3).

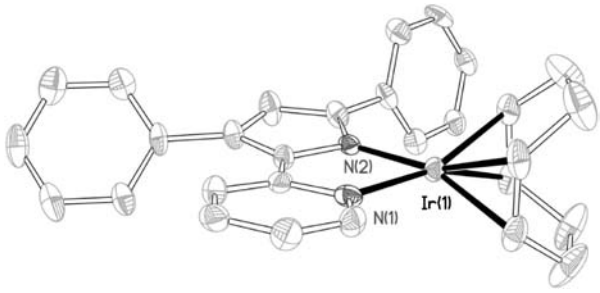

Figure 2. ORTEP diagram of the X-ray crystal structure of **5**. Hydrogen atoms are omitted for clarity. Bond lengths (Å) and angles (deg): Ir1−N1 = 2.087(5), Ir1−N2 = 2.055(5), ∠N1−Ir1−N2 = 79.2(2).

Table 1. Selected Distances (Å) and Angles (deg) for Related Complexes

complex	d(N−M), Å	∠N−M−N, deg
[(bipy)Rh(COD)]PF_6	2.091(4), 2.098(4)	78.6(2)
4	2.080(7), 2.087(7)	78.8(3)
5	2.058(7), 2.082(7)	79.2(3)

Synthesis of (PyPyr)M(CO)$_2$ Complexes. Carbonyl complexes of (PyPyr)Rh and (PyPyr)Ir were of interest as molecules that should help to characterize the electronic properties of the PyPyr ligand. The reaction of **1** with $[RhCl(CO)_2]_2$[51] in benzene provided a modest yield (17%) of (PyPyr)Rh(CO)$_2$ (**6**) after workup and crystallization from a benzene/hexane solvent mixture (Scheme 2). Thus, an alternative route to **6** was sought, and bubbling 1 atm of CO through a solution of **3** in benzene for 1 h quantitatively gave **6** after removal of the volatile components under vacuum (eq 1). Similarly, **4** was treated with 1 atm of CO to quantitatively generate **6** by ^{1}H NMR spectroscopy.

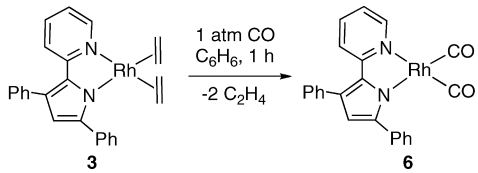

(1)

The analogous Ir carbonyl complex (PyPyr)Ir(CO)$_2$ (**7**) was obtained in low yield (10%) by reaction of **1** with $IrCl(CO)_3$[52] in benzene (eq 2). Complex **7** was isolated from toluene as analytically pure red crystals. An alternative route to **7** is based on treatment of **5** with 1 atm of CO, to quantitatively generate **7** (by ^{1}H NMR spectroscopy).

Scheme 3

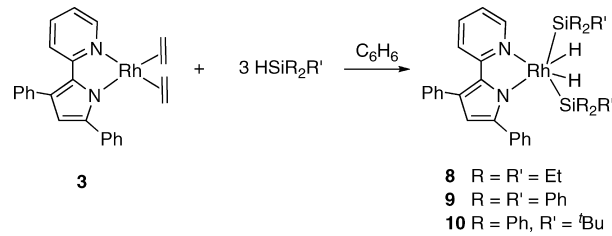

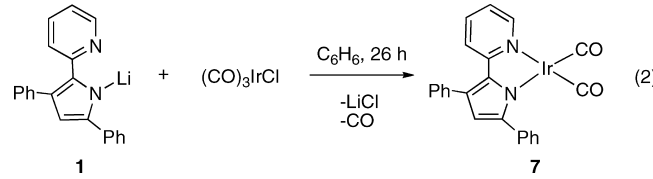

(2)

The IR spectrum of **6** displays two carbonyl stretching frequencies at 2004 and 2067 cm^{-1} and these values are lower than those associated with the related complex [(bipy)Rh(CO)$_2$]ClO_4 (2050, 2108 cm^{-1}).[53] Similarly, the carbonyl stretching frequencies for **7** (1986 and 2050 cm^{-1}) are at lower frequencies than those for [(bipy)Ir(CO)$_2$]ClO_4 (2024, 2089 cm^{-1}).[54] The lower frequency carbonyl stretches of **6** and **7** might reflect more electron-donating properties for PyPyr (vs bipy), but this difference may also be primarily attributed to the difference in charge on the complexes.[55]

Synthesis of (PyPyr)M(H)$_2$(SiR$_3$)$_2$ Complexes. To compare the behaviors of (PyInd)M[42,43] and (PyPyr)M fragments in Si−H activations, reactions of the PyPyr complexes (M = Rh, Ir) with hydrosilanes were explored. Treatment of **3** with three equivs of $HSiEt_3$, $HSiPh_3$, or $HSiPh_2{}^tBu$ in benzene resulted in formation of the 16-electron Rh(V) bis(silyl)dihydrides (PyPyr)Rh(H)$_2$(SiEt$_3$)$_2$ (**8**), (PyPyr)Rh(H)$_2$(SiPh$_3$)$_2$ (**9**), and (PyPyr)Rh(H)$_2$(SiPh$_2{}^t$Bu)$_2$ (**10**), respectively, in good yields (Scheme 3). Under these conditions, the C_2H_4 ligands are lost as the free molecule and as the hydrosilylation product (R_3SiEt). It is worth nothing that **8**−**10** can be generated with only 2 equiv of $HSiR_3$; however, under these reaction conditions, the reaction times exceed 2 d.

The ^{1}H NMR spectra of **8**−**10** in benzene-d_6 exhibit two doublets of doublets in the hydride regions, with observed coupling between the inequivalent hydride ligands and rhodium. For **8**, the hydride resonances appear at −15.43 (J_{RhH} = 25.5 Hz, J_{HH} = 9.5 Hz) and −14.64 ppm (J_{RhH} = 25.0 Hz) and the coupling constants are consistent with classical rhodium hydrides resulting from complete Si−H oxidative addition (Table 2).[56,57] A 2D NOESY experiment revealed that the hydride resonance at −15.43 ppm corresponds to a site *cis* to the pyrrolide group. Although the T_1 value of 0.64 s for both hydrides is not particularly long, it is within the range expected for a classical hydride complex.[58−60] Only one silyl resonance was found in

(51) McCleverty, J. A.; Wilkinson, G. *Inorg. Syn.* **1990**, *28*, 84.
(52) Ginsberg, A. P.; Koepke, J. W.; Sprinkle, C. R. *Inorg. Syn.* **1979**, *19*, 220.
(53) Reddy, G. K. N.; Ramesh, B. R. *J. Organomet. Chem.* **1974**, *67*, 443–447.
(54) Mestroni, G.; Camus, A. *Inorg. Nucl. Chem. Lett.* **1973**, *9*, 261–263.
(55) Goldman, A. S.; Krogh-Jespersen, K. *J. Am. Chem. Soc.* **1996**, *118*, 12159–12166.
(56) Heinrich, H.; Giernoth, R.; Bargon, J.; Brown, J. M. *Chem. Comm.* **2001**, *14*, 1296–1297.
(57) Ezhova, M. B.; Patrick, B. O.; Sereviratne, K. N.; James, B. R.; Waller, F. J.; Ford, M. E. *Inorg. Chem.* **2005**, *44*, 1482–1491.

Table 2. NMR Parameters for Complexes **8**−**11**[(a)]

	^{1}H (ppm)	^{29}Si (ppm)	J_{HH} (Hz)	J_{RhH} (Hz)	J_{SiH} (Hz)	J_{RhSi} (Hz)	T_1 (min) (s)
8	−15.43	78.8	9.5	25.5	4.8	18.8	0.64
	−14.64			25.0	11.6		0.64
9	−13.20	49.1	8.0	22.0	7.4	22.4	0.54
	−11.90			23.0	19.4		0.63
10	−14.64	56.6	9.6	19.2	<0.2	21.8	0.40
	−13.02			24.4	<0.2		0.55
11	−15.80	8.3	2.7		1.9		0.54
	−13.98				1.9		0.67

[(a)] All spectra were acquired in benzene-d_6. T_1 was determined using the null method at 500 MHz.

the ^{29}Si NMR spectrum, at 78.8 ppm. The Si−H coupling constants associated with the hydride ligands in **8**, determined by *J*-resolved ^{1}H,^{29}Si-gradient heteronuclear multiple bond correlation (gHMBC) NMR and ^{29}Si-filtered ^{1}H NMR spectroscopies, were found to have magnitudes of 11.6 Hz for the hydride resonance of −14.64 ppm and 4.8 Hz for the hydride resonance of −15.43 ppm. Generally, J_{SiH} values less than 20 Hz are considered to be 2-bond $^2J_{SiMH}$ couplings in complexes with little or no Si−H interaction; however, this correlation is dependent on the sign of the J_{SiH} coupling constant.[1] Thus, **8** can be viewed as a Rh(V) bis(silyl)dihydride. Similar results were observed for **9** and **10** (Table 2). For **9**, the hydride resonances are observed at −11.90 (J_{RhH} = 23.0 Hz, J_{SiH} = 19.4 Hz) and −13.20 ppm (J_{RhH} = 22.0 Hz, J_{HH} = 8.0 Hz, J_{SiH} = 7.4 Hz). For **10**, the hydride resonances appear at −13.02 (J_{RhH} = 24.4 Hz, J_{HH} = 9.6 Hz) and −14.64 ppm (J_{RhH} = 19.2 Hz), and the J_{SiH} values were too small to be determined (<0.2 Hz).

Attempts to synthesize (PyPyr)Rh(D)$_2$(SiR$_3$)$_2$ complexes gave some insight into the mechanism of these silane activations. Addition of 4 equivs of DSiEt$_3$, DSiPh$_3$, or DSiPh$_2$^{t}Bu to **3** in benzene at 25 °C resulted in partial deuteration of the hydride positions in the bis(silyl)dihydride complexes (by ^{1}H and ^{2}H NMR spectroscopy). For example, addition of 4 equivs of DSiPh$_3$ to **3** in benzene-d_6 gave **9** with 12% H incorporation after 1 h. The incorporation of hydrogen into the hydride positions may occur by the reversible insertion of displaced ethylene into a Rh-D bond. This process would scramble hydrogen between the rhodium complex and free ethylene.

An Ir(V) bis(silyl)dihydride complex, (PyPyr)Ir(H)$_2$(SiPh$_3$)$_2$ (**11**), was obtained by reaction of HSiPh$_3$ with (PyPyr)Ir(COE)$_2$ (COE = cyclooctene), generated in situ by the reaction of [(COE)$_2$IrCl]$_2$[61] with **1** in benzene. The crude product (**11**) was precipitated by the addition of pentane, and pure **11** was isolated in 66% (eq 3). The NMR data for **11** is similar to that of the analogous Rh complexes, with upfield hydride resonances at −13.98 (J_{HH} = 2.7 Hz, T_1 = 0.67 s) and −15.80 ppm (T_1 = 0.54 s) and a small J_{SiH} coupling constant of 1.9 Hz for both hydrides (Table 2). The more upfield-shifted hydride ligand was also found to be *cis* to the pyrrolide, by 2D NOESY NMR spectroscopy.

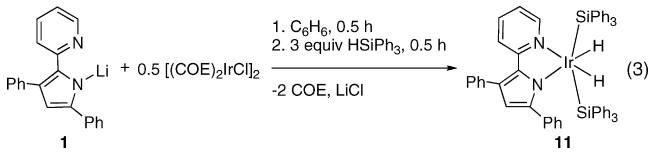

(3)

The solid-state structures of **9** (Figure 3), **10** (Figure 4), and **11** (Figure 5) were determined by single crystal X-ray crystallography. These formally 16 electron complexes exhibit similar

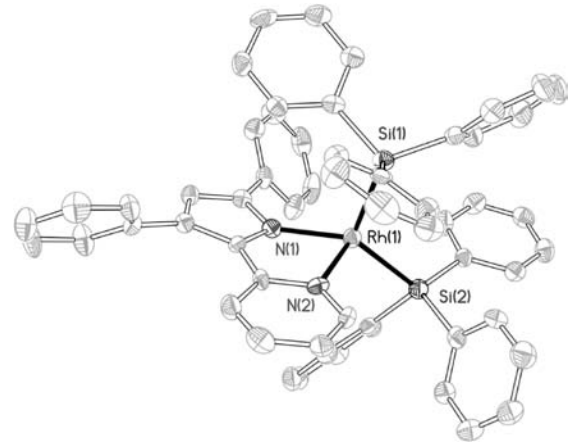

Figure 3. ORTEP diagram of the X-ray crystal structure of **9**; the metal hydrides were not located from the difference Fourier map. Hydrogen atoms are omitted for clarity. Bond lengths (Å) and angles (deg): Rh1−N1 = 2.039(4), Rh1−N2 = 2.154(5), Rh1−Si1 = 2.318(2), Rh1−Si2 = 2.339(2), ∠N1−Rh1−N2 = 78.0(1), ∠Si1−Rh1−Si2 = 115.00(6), ∠N1−Rh1−Si1 = 106.6(1), ∠N1−Rh1−Si2 = 136.0(1), ∠N2−Rh1−Si1 = 100.3(1), and ∠N2−Rh1−Si2 = 107.2(1).

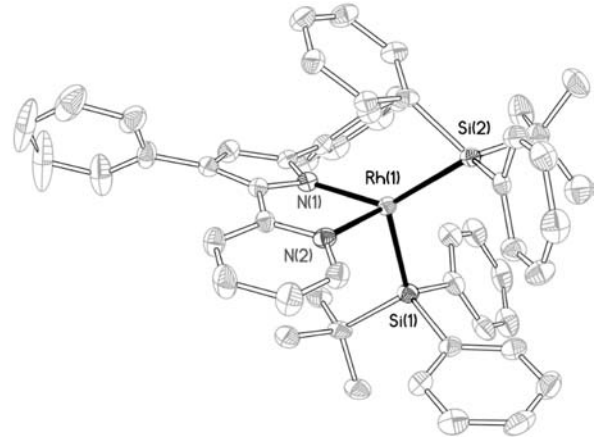

Figure 4. ORTEP diagram of the X-ray crystal structure of **10**; the metal hydrides were not located from the difference Fourier map. Hydrogen atoms are omitted for clarity. Bond lengths (Å) and angles (deg): Rh1−N1 = 2.039(2), Rh1−N2 = 2.168(2), Rh1−Si1 = 2.3420(9), Rh1−Si2 = 2.3664(9), ∠N1−Rh1−N2 = 78.96(9), ∠Si1−Rh1−Si2 = 116.62(3), ∠N1−Rh1−Si1 = 103.99(7), ∠N1−Rh1−Si2 = 136.62(7), ∠N2−Rh1−Si1 = 101.67(7), and ∠N2−Rh1−Si2 = 105.68(7).

geometries that are unusual for six-coordinate, group 9 metal compounds. The observed coordination geometry for these complexes is greatly distorted from an octahedron, such that the Si-M-Si angles are 115.00(6)°, 116.62(3)°, and 116.10(4)°, for **9**−**11**, respectively. A similar Si−Rh−Si distortion angle of 107.9° was observed for Cp*RhH$_2$(SiEt$_3$)$_2$.[28] Also, the Rh−Si bond distance of 2.379(2) Å for Cp*RhH$_2$(SiEt$_3$)$_2$ is similar to the corresponding distances in **9** (2.318(2), 2.339(2) Å) and **10** (2.3149(9), 2.366(1) Å).

These structures are also similar to that of (PyInd)Ir(H)$_2$(SiPh$_2$Me)$_2$.[42] For (PyInd)Ir(H)$_2$(SiPh$_2$Me)$_2$, the Ir−Si bond

(58) Hamilton, D. G.; Crabtree, R. H. *J. Am. Chem. Soc.* **1988**, *110*, 4126–4133.
(59) Desrosiers, P. J.; Cai, L.; Lin, Z.; Richards, R.; Halpern, J. *J. Am. Chem. Soc.* **1991**, *113*, 4173–4184.
(60) Ammann, C.; Pregosin, P. S. *Magn. Reson. Chem.* **1988**, *26*, 236–238.
(61) van der Ent, A.; Onderdelinden, A. L. *Inorg. Syn.* **1990**, *28*, 90.

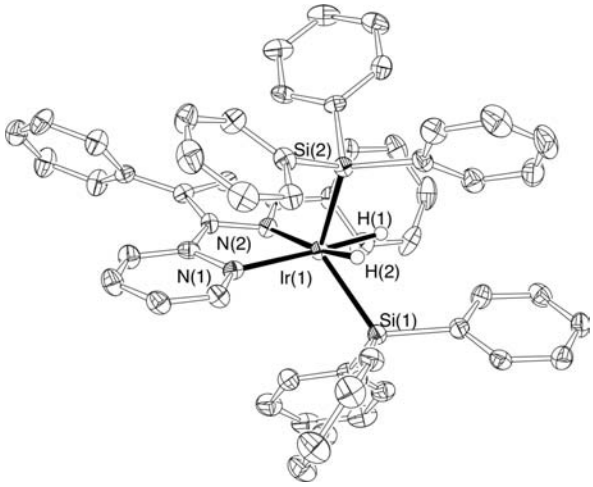

Figure 5. ORTEP diagram of the X-ray crystal structure of **11**. Hydrogen atoms, excluding metal hydrides, are omitted for clarity. Bond lengths (Å) and angles (deg): Ir1−N1 = 2.130(4), Ir1−N2 = 2.039(4), Ir1−Si1 = 2.337(1), Ir1−Si2 = 2.329(1), Ir1−H1 = 1.57(3), Ir1−H2 = 1.74(1), ∠N1−Ir1−N2 = 78.1(1), ∠Si1−Ir1−Si2 = 116.10(4), ∠N1−Ir1−Si1 = 106.3(1), ∠N1−Ir1−Si2 = 99.7(1), ∠Si1−Ir1−H1 = 75(1), ∠Si1−Ir1−H2 = 76(1), ∠Si2−Ir1−H1 = 78(1), ∠Si2−Ir1−H2 = 58(1), ∠N2−Ir1−Si1 = 131.5(1), and ∠N2−Ir1−Si2 = 110.4(1).

distances of 2.326(1) Å and 2.338(1) Å are very close to the values for **11** (2.329(1), 2.337(1) Å). Furthermore, (PyInd)Ir-$(H)_2(SiPh_2Me)_2$ exhibits a small Si−Ir−Si bond angle of 105.7° which may be compared to that observed for **11** (116.10(4)°). As previously noted,[62] six-coordinate d^4 complexes may exhibit strong distortions from octahedral geometry. In these cases, the distortion toward an appropriate bicapped tetrahedron geometry appears to be driven by the strong *trans*-influencing nature of the silyl groups, which prefer to avoid a *trans* arrangement that would force them to directly compete for overlap with a metal-based orbital. The N-M-Si angles associated with the pyrrolide nitrogen, of 106.6(1)° and 136.0(1)° for **9**, 103.99(7)° and 136.62(7)° for **10**, and 110.4(1)° and 131.5(1)° for **11**, indicate an additional type of distortion from octahedral geometry. As observed for $(PyInd)Ir(H)_2(SiPh_2Me)_2$,[42] the silyl groups of **9**−**11** lean toward the pyridyl side of the PyPyr ligand. Unfortunately, the hydride ligands in these complexes could only be located from the difference Fourier maps for **11**. The hydride ligands in complex **11** complete the square plane with Ir−H distances of 1.57(3) and 1.74(1) Å. Furthermore, the smallest Si−H distance (between Si2 and H2) is 2.04 Å, indicating very little interaction between the two atoms. However, weak residual Si···H interactions[63] or secondary interactions between the silicon and hydrogen atoms (SISHA), as described by Sabo-Etienne,[64] cannot be ruled out based on these Si−H distances without a full computational analysis. For **9** and **10**, the hydride ligands are presumed to complete an approximate square planar geometry with the (PyPyr)M fragments similar to **11**. The absence of intramolecular Si−H interactions is indicated by the regular bond angles about silicon (for **9**, Rh−Si1−C: 107.4(2), 105.6(2), 118.9(2) and Rh−Si2−C: 114.2(2), 120.1(2), 91.7(2)).

Reaction of $H_2Si^tBu_2$ with (PyPyr)Rh(C_2H_4)$_2$. Addition of 1 or 2 equiv of $H_2Si^tBu_2$ to **3** in benzene resulted in formation of

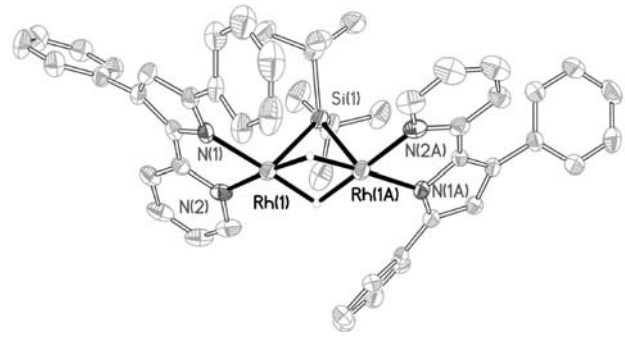

Figure 6. ORTEP diagram of the X-ray crystal structure of **12**. Hydrogen atoms, excluding metal hydrides, are omitted for clarity. Bond lengths (Å) and angles (deg): Rh1−N1 = 2.037(3), Rh1−N2 = 2.048(3), Rh1−Si1 = 2.279(1), Rh1−H1 = 1.67(3), ∠N1−Rh1−N2 = 78.0(1), ∠Si1−Rh1−H1 = 74(1), ∠N1−Rh1−Si1 = 108.16(9), ∠N1−Rh1−H1 = 105(1), ∠N2−Rh1−Si1 = 107.08(9), and ∠N2−Rh1−H1 = 176(1).

the dimeric Rh complex (PyPyr)Rh(μ-H)$_2$(μ-Si^{t}Bu$_2$)Rh(PyPyr) (**12**) in 32% yield (eq 5). The ^{1}H NMR spectrum confirms the presence of a bridging hydride by the upfield triplet observed at −24.25 ppm (J_{RhH} = 32.4 Hz). The ^{29}Si NMR spectrum also indicates a bridging silylene ligand with the presence of a downfield resonance at 252.8 ppm. The solid-state structure of **12** was determined by X-ray crystallography (Figure 6). Complex **12** exhibits Rh−H (1.67 Å) and Rh−Si (2.279 Å) bond distances that are typical for bridging hydride and silylene ligands in rhodium complexes.[65] The coordination geometry about the equivalent rhodium atoms (related by a 2-fold axis) is approximately a square-based pyramid, with the silicon atom in the apical position.

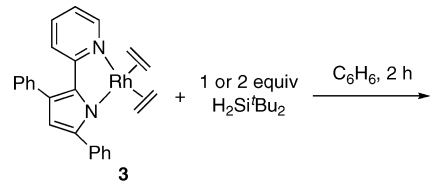

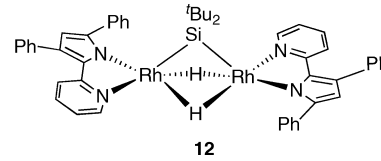

(4)

Silane Exhange of (PyPyr)Rh(H)$_2$(SiR$_3$)$_2$. As a further probe of reactivity patterns in high valent silyl hydride complexes such as **8**−**11**, the exchange of free silane into these complexes was examined. In principle, such reactions should reveal insights into bond activation processes that involve (PyPyr)M (M = Rh, Ir) fragments. A fundamental question concerns the mechanism of Si−H activation by complexes such as (PyPyr)Rh(H)$_2$(SiR$_3$)$_2$, and the intriguing possibilities of (1) an associative process for a six-coordinate species, or (2) a dissociative mechanism involving a 14-electron four-coordinate Rh(III) intermediate.

Addition of free tertiary silanes to **8**−**10** revealed that silane exchange reactions are favored when less sterically demanding silyl groups are introduced at the metal center. When 2 equiv of $HSiEt_3$ was added to **9** or **10**, **8** was quantitatively generated (by ^{1}H NMR spectroscopy). Interestingly, addition of 1 equiv of $HSiEt_3$ to **10** gave two new doublet of doublet resonances in

(62) Kubacek, P.; Hoffmann, R. *J. Am. Chem. Soc.* **1981**, *103*, 4320–4332.
(63) Vyboishchikov, S. F.; Nikonov, G. I. *Organometallics* **2007**, *26*, 4160–4169.
(64) Lachaize, S.; Sabo-Etienne, S. *Eur. J. Inorg. Chem.* **2006**, 2115–2117.
(65) Fryzuk, M. D.; Rosenberg, L.; Rettig, S. J. *Organometallics* **1996**, *15*, 2871–2880.

the hydride region of the ^{1}H NMR spectrum. These resonances, at −13.6 (J_{RhH} = 26.0 Hz, J_{HH} = 9.8 Hz) and −15.3 ppm (J_{RhH} = 22.2 Hz, J_{HH} = 9.8 Hz), are consistent with formation of the mixed silyl species (PyPyr)Rh(H)$_2$(Si^{t}BuPh$_2$)(SiEt$_3$) (eq 5). Addition of a second equiv of HSiEt$_3$ to (PyPyr)Rh(H)$_2$(Si^{t}BuPh$_2$)(SiEt$_3$) quantitatively gave **8** after 1 d at 25 °C (by ^{1}H NMR spectroscopy). Similarly, addition of 1 equiv of HSiEt$_3$ to a solution of **9** in benzene quantitatively generated (PyPyr)Rh(H)$_2$(SiPh$_3$)(SiEt$_3$) and 1 equiv of HSiPh$_3$. Conversion to **8** was observed after addition of a second equiv of HSiEt$_3$ to the reaction mixture for 1 d at 25 °C.

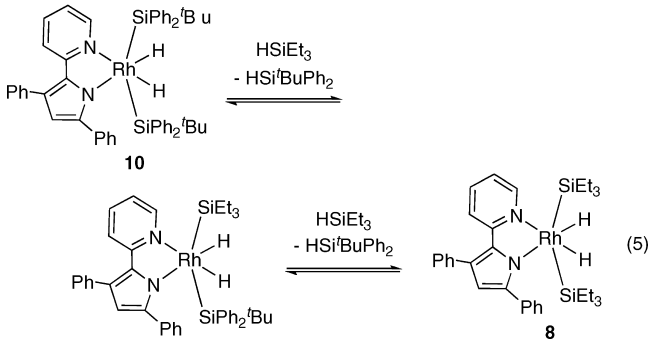

(5)

In a similar manner, silane exchange with HSiPh$_3$ was also investigated. Addition of 2 equiv of HSiPh$_3$ to a benzene solution of **10** quantitatively gave **9** after 1 d at 25 °C (by ^{1}H NMR spectroscopy). In contrast, addition of 2 equiv of HSiPh$_3$ to a benzene solution of **8** did not produce the silane exchange product **9** after 1 d at 25 °C, and **8** remained unchanged by these reaction conditions. This trend implies that for the silane exchange to occur, a silane smaller in size must be incorporated into the metal-containing product (that is HSiEt$_3$ will displace both HSi^{t}BuPh$_2$ and HSiPh$_3$, and the latter will displace HSi^{t}BuPh$_2$).

To investigate the mechanism of silane exchange in the reaction of **10** with HSiEt$_3$, a kinetic study was initiated. At 323 K in benzene-d_6, the concentration dependence for each substrate was determined by monitoring the reaction rate under pseudo first order conditions. To determine the reaction order in **10**, the silane exchange was followed under 10−100 equiv of excess HSiEt$_3$. Under these conditions, a first order dependence on [**10**] was observed. In a similar manner, the reaction order in HSiEt$_3$ was determined by following the silane exchange of **10** with HSiEt$_3$ in the presence of 10−100 equiv of excess [**10**]. No dependence on [HSiEt$_3$] was observed, and the overall rate expression takes the form: rate = k_{obs}[**10**] (for the first silane exchange). The change in k_{obs} as a function of temperature was also monitored by ^{1}H NMR spectroscopy over the temperature range of 236.2 to 275.8 K in toluene-d_8. A linear fit of an Eyring plot (Figure 7) was used to determine the entropy ($\Delta S^{\ddagger}$) and enthalpy ($\Delta H^{\ddagger}$) of activation for the first silane exchange of eq 5. The $\Delta H^{\ddagger}$ and $\Delta S^{\ddagger}$ values were determined to be 21.3(5) kcal/mol and 10.8(3) e.u., respectively. Thus, the rate law and Eyring analysis are consistent with a rate determining step in the silane exchange mechanism consisting of the reductive elimination of HSi^{t}BuPh$_2$ to generate a 14-electron Rh(III) silylhydride. This Rh(III) intermediate would then undergo rapid oxidative addition of silane to reform a 16-electron Rh(V) bis(silyl)dihydride (eq 6).

This kinetic behavior is consistent with that observed for the activation of benzene by the 18 electron complex Cp*(PMe$_3$)Ir(cyclohexyl)(H), in that it involves the rate-limiting

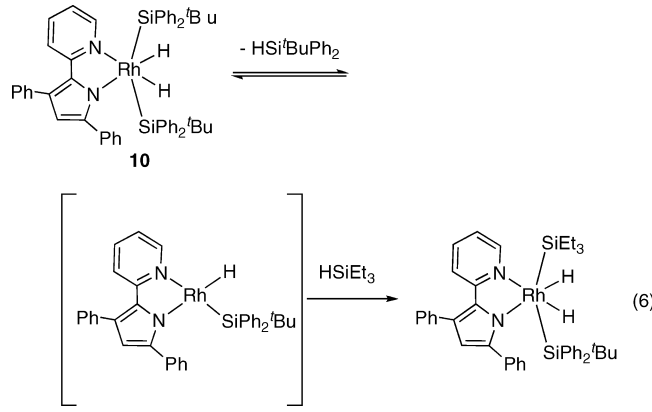

(6)

reductive elimination of cyclohexane.[66] The rate of formation of the benzene activation complex is independent of benzene concentration. In this system, the 16 electron intermediate Cp*(PMe$_3$)Ir appears to react directly with benzene to give the final product, Cp*(PMe$_3$)Ir(Ph)(H). Interestingly, the related bond activation of eq 6 appears to proceed through a formally 14 electron intermediate. An analogous species, (PyInd)Rh(H)(SiEt$_3$), has been proposed as a key intermediate that oxidatively adds chlorobenzene in the catalytic dehydrochlorinative silylation of haloarenes.[42]

Addition of 2 equiv of DSiEt$_3$ to **10** in benzene-d_6 gave **8** with the same amount of partial deuteration at both hydride positions, as determined by ^{1}H and ^{2}H NMR spectroscopy. It is also worth noting that no solvent (benzene) activation was observed during the course of silane exchange.

Thermolysis of (PyPyr)Rh(H)$_2$(Si^{t}BuPh$_2$)$_2$. Given the dissociative nature of silane exchange into complex **10**, attempts were made to observe loss of HSi^{t}BuPh$_2$ under conditions that might allow observation of a Rh(III) intermediate. Heating a solution of **10** in benzene to 50 °C for 1 h resulted in loss of HSi^{t}BuPh$_2$ and formation of [(PyPyr)Rh(μ-H)(Si^{t}BuPh$_2$)]$_2$ (**13**) (Scheme 4). An upfield triplet at −21.99 ppm (J_{RhH} = 33.6 Hz) in the ^{1}H NMR spectrum confirms that the hydride is bridging two Rh centers while the ^{29}Si resonance at 33.1 ppm supports the presence of a nonbridging silyl group.[1] Complex **13** can be viewed as a dimer of the 14-electron Rh(III) intermediate in the silane exchange path (eq 6). Interestingly, the formation of **13** occurs on the same time scale as the first silane exchange of **10** with HSiEt$_3$ at 50 °C; however, small impurities that form during the thermolysis of **10** did not allow for a kinetic analysis. A direct synthesis of **13** from **3** was achieved by addition of 1

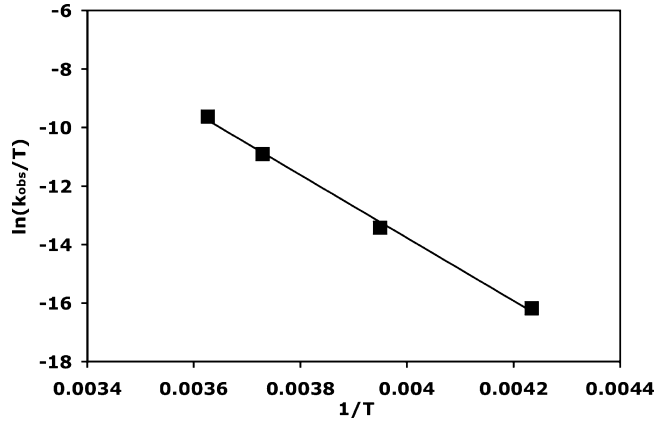

Figure 7. Eyring plot for the conversion of **10** to (PyPyr)Rh(H)$_2$(Si^{t}BuPh$_2$)(SiEt$_3$).

Scheme 4

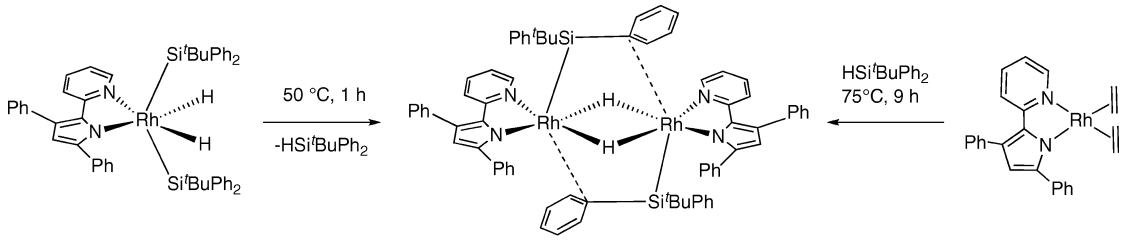

equiv of HSi^{t}BuPh$_2$ to **3** in benzene, followed by heating for 9 h at 75 °C to give the product in good yield (66%).

The solid-state structure of **13** was determined by X-ray crystallographic analysis (Figure 8). As predicted by NMR spectroscopy, the silyl group lies in the apical position relative to the (PyPyr)RhH plane, with N−Rh−Si bond angles of 99.2(1)° and 97.3(1)° and a Si−Rh−H bond angle of 88(1)°. The tetrahedral geometry about the silicon center and the long Si−H distances (>2.71 Å) indicate that there is no Si−H interaction. Interestingly, the phenyl substituents of the silyl groups are oriented such that they appear to be coordinated to the rhodium centers. The resulting C_{ipso}−Rh distance of 2.82 Å is consistent with a weak bonding interaction. This interaction is similar to that observed for another rhodium complex, [Rh(1,3-dimesityl-3,4,5,6-tetrahydropyrimidin-2-yli-dene)(COD)][PF], which possesses an electron-donating interaction between an *ipso* carbon and the rhodium center, with C_{ipso}−Rh distances of 2.353 Å and 2.346 Å.[67] For comparison, the iridium analogue (**11**) remained unchanged after it was heated in mesitylene to 160 °C for 2 d (by ^{1}H NMR spectroscopy).

Addition of Lewis Bases to (PyPyr)Rh(H)$_2$(SiPh$_3$)$_2$. Reactions with Lewis bases were examined to further explore the lability of the bis(silyl)dihydrides. Addition of 1 equiv PPh_3 to **9** in benzene resulted in displacement of 1 equiv of $HSiPh_3$ within 1 h to generate (PyPyr)Rh(H)(SiPh$_3$)(PPh$_3$) (**14**) in 73% yield (eq 7). The ^{1}H NMR spectrum of **14** reveals one hydride resonance at −12.94 ppm as a doublet of doublets (J_{RhH} = 28.8 Hz, J_{PH} = 20.4 Hz) while the ^{31}P{^{1}H} NMR spectrum exhibits a doublet at 42.27 ppm (J_{RhP} = 138 Hz). Furthermore, a ^{1}H,^{29}Si gHMBC experiment gave one ^{29}Si resonance at 32.2 ppm. The coordination geometry about the Rh center was determined by 2D NOESY to be a square-based pyramid that was confirmed by single crystal X-ray crystallography (Figure 9). The silyl group occupies the apical position, and the Rh−Si bond distance is 2.294(1) Å. Relative to **9** − **11**, only a small distortion is observed in the silyl ligand (N−Rh−Si angles of 98.5(1)° and 106.4(1)°, versus 135.9(1)°, 107.2(1)°, 106.6(1)° and 100.2(1)° for **9**). The phosphine substituent occupies the position *trans* to the pyrrolide group, due to its weaker *trans* influence relative to a hydride or a silyl ligand. Other Lewis bases that are stronger sigma donors than aryl phosphines, such as CO and xylylisocyanide, displace both silanes to give intractable mixtures of products.

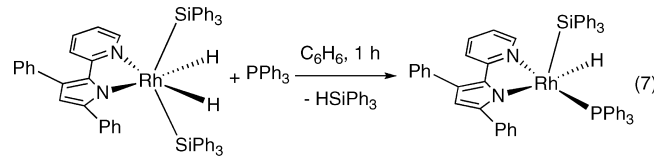

(7)

An attempt was made to examine the kinetics of the silane displacement reaction of eq 7, and this showed that this reaction proceeds very rapidly at 25 °C (within 5 min by ^{1}H NMR spectroscopy) upon addition of PPh_3 to a C_6D_6 solution **9**. Thus, a full mechanistic analysis was not completed. It is noteworthy that this reaction proceeds much more rapidly than the silane exchange reaction of **10** with $HSiEt_3$, which occurs via a rate determining elimination of HSi^{t}BuPh$_2$. These results, in combination with the observation that **10** does not undergo rapid reductive elimination of $HSiPh_3$ in the absence of PPh_3 at 25

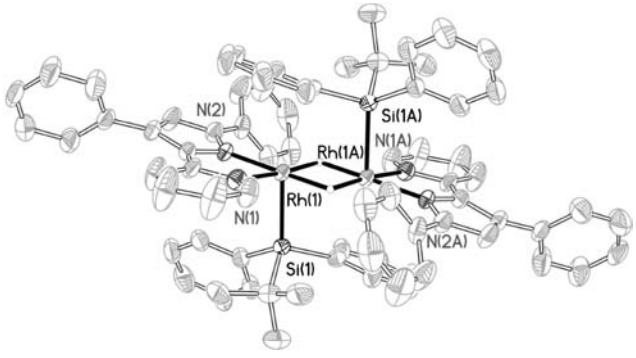

Figure 8. ORTEP diagram of the X-ray crystal structure of **13**. Hydrogen atoms, excluding metal hydrides, and disordered THF molecule are omitted for clarity. Bond lengths (Å) and angles (deg): Rh1−N1 = 2.036(4), Rh1−N2 = 2.040(3), Rh1−Si1 = 2.340(1), Rh1−H1 = 1.70(4), ∠N1−Rh1−N2 = 78.6(1), ∠Si1−Rh1−H1 = 88(1), ∠N1−Rh1−Si1 = 97.3(1), ∠N1−Rh1−H1 = 174(1), ∠N2−Rh1−Si1 = 99.2(1), and ∠N2−Rh1−H1 = 101(1).

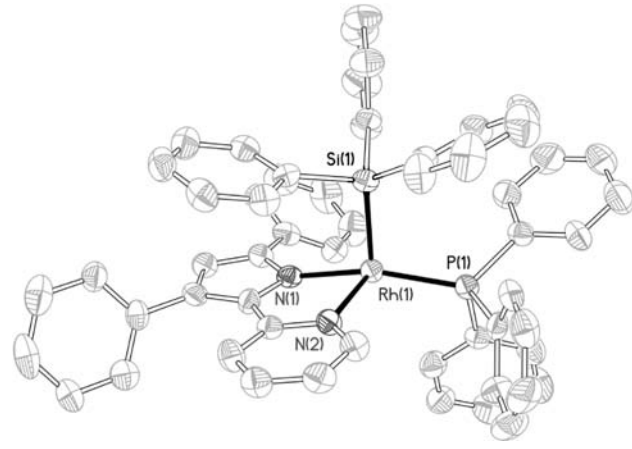

Figure 9. ORTEP diagram of the X-ray crystal structure of **14**. Hydrogen atoms, excluding metal hydrides, and benzene molecule are omitted for clarity. Bond lengths (Å) and angles (deg): Rh1−N1 = 2.072(4), Rh1−N2 = 2.168(4), Rh1−Si1 = 2.294(1), Rh1−P1 = 2.239(1), ∠N1−Rh1−N2 = 77.6(1), ∠Si1−Rh1−P1 = 100.10(6), ∠N1−Rh1−Si1 = 98.5(1), ∠N1−Rh1−P1 = 160.2(1), ∠N2−Rh1−Si1 = 97.7(1), and ∠N2−Rh1−P1 = 106.4(1).

Table 3. Hydrosilylation Catalysis[a]

Entry	Olefin/Alkyne	Silane	Products	Yield (%) cat. **3**	Yield (%) cat. **6**
1	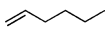	$HSiEt_3$	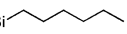	0	0
2	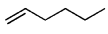	$HSiPh_3$	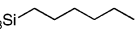	> 95	0
3		$HSiPh_3$		0	0
4		$HSiEt_3$	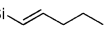	50	50
				41	41
5		$HSiPh_3$	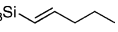	8	5
				87	89
6		$HSiEt_3$	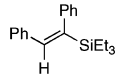	> 95	> 95
7		$HSiPh_3$	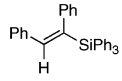	> 95	> 95
8		$HSiPh_3$	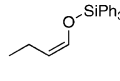	79	62
			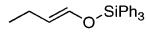	21	38
9		$HSiEt_3$	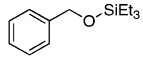	> 95[b]	> 95[b]
10		$HSiPh_3$	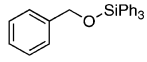	> 95[b]	> 95[b]

[a] Reactions were conducted with 0.1 mmol of substrate and silane and 5 mol % of catalyst in 1 mL of C_6D_6 at 60 °C for 16 h. Yield and stereochemistry were determined by ^{1}H NMR relative to an internal standard and confirmed by GCMS. [b] Reactions was conducted at 25 °C for 4 h.

°C in C_6D_6, suggest that the mechanisms for silane exchange and silane displacement by PPh_3 may not proceed through a common intermediate.

Catalytic Hydrosilylation. The ease of Si−H activations in reactions of silanes with **3** prompted an investigation of hydrosilylation catalysis by these complexes. Compounds **3** and **6** were found to be good hydrosilylation catalysts for an array of simple olefins and alkynes, with tertiary silanes. Catalytic runs involved addition of 5 mol % of the catalyst to a solution of the silane and either olefin or alkyne in 1 mL of C_6D_6. The solution was sealed and heated for 16 h at 60 °C and the reactions were monitored by ^{1}H NMR spectroscopy. The products were isolated, and their identities were confirmed and quantified by ^{1}H NMR spectroscopy and GCMS analysis. The hydrosilylation of 1-hexene was found to proceed with **3** as the catalyst and $HSiPh_3$ as the silane (Table 3, Entries 1,2). A more sterically encumbered olefin, *t*-butylethylene, gave no hydrosilylation products with either catalyst (Table 3, Entry 3). For alkynes, the hydrosilylation of 1-pentyne was facilitated by both **3** and **6**, and either $HSiEt_3$ or $HSiPh_3$ as the silane, in good yields (Table 3, Entries 4,5). However, modest selectivity (cis/trans ratios: 41:50 for $HSiEt_3$ with **3** or **6**; 87:8 for $HSiPh_3$ with **3**, and 89:5 for $HSiPh_3$ with **6**) was observed for both catalysts. For the disubstituted alkyne diphenylacetylene, hydrosilylation with either **3** or **6** as the catalyst and $HSiEt_3$ or $HSiPh_3$ as the silane gave only the *cis* addition product (Table 3, Entries 6,7). Hydrosilylation of the α,β-unsaturated aldehyde, crotonaldehyde, gave 1,4 addition products in good yield with moderate selectivity under mild reaction conditions (4 h at 25 °C, Table 3, Entry 8). The hydrosilylation of benzaldehyde, with either **3** or **6** as a catalyst and $HSiEt_3$ or $HSiPh_3$ as the silane, also proceeded under these less harsh conditions to give the silyl ether product in >95% yield (Table 3, Entries 9,10). These catalytic hydrosilylation results are comparable to those obtained with the known catalyst $(PR_3)_3RhCl$.[68,69]

As mentioned above, the complex $(PyInd)Rh(C_2H_4)_2$ catalyzes the dehydrochlorinative silylation of chlorobenzene under mild conditions.[42] Treatment of chlorobenzene, $LiN(^iPr)_2$, and $HSiEt_3$ with 5 mol % of **3** or **6** at 60 °C for 16 h did not give dehydrochlorinative silylation products. Instead, arene dechlorination was observed to give benzene and $ClSiEt_3$ (eq 8), by ^{1}H NMR spectroscopy and GCMS. Other bases ($LiN(SiMe_3)_2$ and KO^tBu) gave only dechlorinative products as did changing the silane (to $HSiPh_3$) and the haloarene (to PhI).

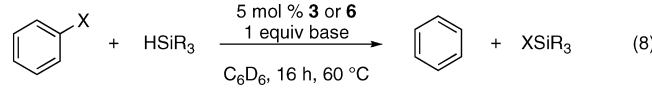

R = Et, Ph
X = Cl, I
base = $LiN(^iPr)_2$, KO^tBu, $LiN(SiMe_3)_2$

Concluding Remarks

This work demonstrates that rhodium and iridium complexes supported by the chelating, pyridyl-pyrollide ligand PyPyr participate in a number of Si−H bond activation processes, both stoichiometrically and catalytically. This system is therefore much like that based on related pyridyl-indolide ligands, (PyInd)M (M = Rh, Ir).[42] For both types of complexes, double silane activations are observed to give unusual six-coordinate, 16-electron, pentavalent complexes of the type $(L_2)MH_2(SiR_3)_2$ that are severely distorted from an octahedral geometry. This distortion, and the low formal electron count, undoubtedly result from the tendency for ligands with a strong *trans* influence (e.g., hydride and silyl) to avoid mutually *trans* arrangements.[42] Interestingly, whereas the (PyInd)M complexes have been found to catalyze Si−C coupling reactions between hydrosilanes and arylchlorides, this reactivity is not observed for the analogous (PyPyr)M species under comparable conditions. On the basis of experiments reported here, it seems that bond activations by these $(L_2)MH_2(SiR_3)_2$ complexes may proceed via interesting 14-electron intermediates of the type $(L_2)MH(SiR_3)$. An analogous 14 electron complex "(PCP)Ir" has been proposed as an intermediate in catalytic alkane-transfer dehydrogenations.[70] In the latter system, the 14 electron intermediate (PCP)Ir is thought to be generated by loss of $CH_3CH_2{}^tBu$ from the proposed intermediate $(PCP)Ir(H)(CH_2CH_2{}^tBu)$.

(66) Buchanan, J. M.; Stryker, J. M.; Bergman, R. G. *J. Am. Chem. Soc.* **1986**, *108*, 1537–1550.
(67) Zhang, Y.; Wang, D.; Wurst, K.; Buchmeiser, M. R. *J. Organomet. Chem.* **2005**, *690*, 5728–5735.
(68) Brady, K. A.; Nile, T. A. *J. Organomet. Chem.* **1981**, *206*, 299–304.
(69) Ojima, I.; Nihonyanagi, M.; Kogure, T.; Kumagai, M.; Horiuchi, S.; Nakatsugawa, K. *J. Organomet. Chem.* **1975**, *94*, 449–461.
(70) Renkema, K. B.; Kissin, Y. V.; Goldman, A. S. *J. Am. Chem. Soc.* **2003**, *125*, 7770–7771.

In summary, rhodium and iridium complexes of the types described above appear to be potentially useful as catalysts that employ bond activations in the conversion of substrates. Since this reactivity depends, at least to some extent, on the nature of the chelating, ancillary ligand, future efforts will focus on optimizations of bond activation processes via modifications of such ligands.

Experimental Section

General Procedures. All experiments were conducted under nitrogen using standard Schlenk techniques or in a Vacuum Atmospheres drybox. Nondeuterated solvents were distilled under N_2 from appropriate drying agents and stored in PTFE-valved flasks. Deuterated solvents (Cambridge Isotopes) were vacuum-transferred from appropriate drying agents.

All olefins, alkynes, haloarenes, PPh_3 and aldehydes were purchased from Aldrich and dried over appropriate drying agents. Ethylene and carbon monoxide were obtained from Praxair and were used as received. The compounds 3,5-diphenyl-2-(2-pyridyl)pyrrole (PyPyrH),[44] $IrCl(CO)_3$,[52] and $LiN(SiMe_3)_2$[71] were synthesized according to literature procedures. Rhodium and iridium precursors were prepared according to literature procedures.[47−49,51,52,61] Silanes were purchased from Gelest or Aldrich and used without further purification.

Analytical Methods. ^1H, ^2H, ^{29}Si $\{^1H\}$, ^{31}P, and $^{13}C\{^1H\}$ NMR spectra were recorded using Bruker AVB 400, AV-500 or DRX 500 spectrometers equipped with a 5 mm BB probe. Spectra were recorded at room temperature and referenced to the residual protonated solvent for ^1H NMR spectrum or to an internal tetramethylsilane for the ^{29}Si NMR spectrum. $^{31}P\{^1H\}$ NMR spectra were referenced relative to 85% H_3PO_4 external standard ($\delta = 0$). $^{13}C\{^1H\}$ NMR spectra were calibrated internally with the resonance for the solvent relative to tetramethylsilane. FT-IR spectra were recorded for samples as Nujol mulls on KBr plates using a Mattson FTIR 3000 spectrometer at a resolution of 4 cm^{-1}. Elemental analyses were performed by the College of Chemistry Microanalytical Laboratory at the University of California, Berkeley. Identities of organic products were confirmed by ^1H NMR spectroscopy and by GCMS, using an Agilent Technologies 6890N GC system with an HP-5MS column.

Li(PyPyr) (1). Solid $LiN(SiMe_3)_2$ (0.294 g, 1.76 mmol) was added to a stirred, room-temperature solution of 3,5-diphenyl-2-(2-pyridyl)pyrrole, (PyPyr)H, (0.521 g, 1.76 mmol) in ca. 8 mL of benzene. The reaction mixture was allowed to stir at ambient temperature for 10 h. After removing the volatile materials under reduced pressure, hexane (ca. 3 mL) was added to the reaction mixture before filtering it through a glass frit. The solids were washed with hexanes (5 × 3 mL), and dried under vacuum (0.402 g, 75.6%). ^1H NMR (C_6D_6, 500 MHz): δ 6.2−7.8 (br, m, overlaps with C_6D_6). ^1H NMR (CD_3CN, 500 MHz): δ 6.49 (br, 1H), 6.80 (br, 1H), 7.02 (br, 1H), 7.16−7.69 (overlapping multiplets, 9H), 7.71 (d, $^3J_{HH}$ = 7.6 Hz, 2H), 8.21 (br, 1H). Anal. Calcd for $C_{21}H_{15}N_2Li$: C, 83.44; H, 5.00; N, 9.27. Found: C, 83.43; H, 5.17; N, 8.89.

Alternative Synthesis of Li(PyPyr) (1). A 2.2 mL hexane solution of butyllithium (1.6 M, 3.5 mmol) was added to a stirred, room-temperature solution of 3,5-diphenyl-2-(2-pyridyl)pyrrole (1.01 g, 3.42 mmol) in ca. 10 mL of benzene. The reaction mixture was allowed to stir at ambient temperature for 40 h. The reaction mixture was dried under vacuum before it was washed with hexanes (10 mL), and dried under vacuum to afford a yellow solid (0.944 g, 91.3%). The ^1H NMR spectrum of this product is identical to that of the synthesis given above.

Generation of a Mixture of (PyPyr)H, $[(C_2H_4)_2RhCl]_2$, and (PyPyrH)RhCl(C_2H_4) (2). To a suspension of $[(C_2H_4)_2RhCl]_2$ (0.053 g, 0.14 mmol) in 5 mL of toluene, (PyPyr)H (0.081 g, 0.27 mmol) was added and the resulting mixture was stirred to give an orange solution which precipitated a yellow solid. After 3 h of stirring at room temperature, 1 mL of pentane was added to facilitate complete precipitation. The filtrate was decanted, and the solids were dissolved in 1.5 mL of toluene and then precipitated with pentane three times to give a yellow powder (0.050 g, 52% crude yield). ^1H NMR (C_6D_6, 500 MHz): δ 2.10−2.39 (m, 4H), 3.30−3.55 (m, 4H), 6.07 (t, $^3J_{HH}$ = 6.2 Hz, 1H), 6.31 (t, $^3J_{HH}$ = 7.3 Hz, 1H), 6.77 (m, 1H), 6.88−7.40 (m, overlapping with benzene-d_6), 8.19 (d, $^3J_{HH}$ = 8.0 Hz, 2H), 8.47 (d, $^3J_{HH}$ = 4.9 Hz, 1H), 12.44 (br, 1H). Anal. Calcd for $C_{25}H_{24}N_2ClRh$: C, 61.18; H, 4.93; N, 5.71. Found: C, 61.26; H, 4.95; N, 5.85.

(PyPyr)Rh(C_2H_4)$_2$ (3). Solid **1** (1.25 g, 4.13 mmol) was added to a stirred, room-temperature solution of $[(C_2H_4)_2RhCl]_2$ (0.805 g, 2.08 mmol) in 50 mL of benzene. The reaction mixture was allowed to stir at ambient temperature for 12 h, and then it was filtered. Volatile materials were removed under reduced pressure, and **3** was isolated as an analytically pure brown powder (1.82 g, 97.1%). ^1H NMR (C_6D_6, 500 MHz): δ 2.06 (d, J_{RhH} = 11.0 Hz, 2H, *CH*$_2$), 2.86 (d, J_{RhH} = 11.0 Hz, 2H, *CH*$_2$), 3.07 (br, 4H, *CH*$_2$), 5.91 (t, J_{HH} = 6.4 Hz, 1H), 6.46 (t, J_{HH} = 8.4 Hz, 1H), 6.47 (s, 1H), 6.78 (d, J_{HH} = 5.6 Hz, 1H), 6.97−7.28 (m, overlapping with benzene-d_6), 7.55 (d, J_{HH} = 7.6 Hz, 2H), 7.70 (d, J_{HH} = 7.6 Hz, 2H). ^1H NMR (toluene-d_8, 500 MHz): 2.05 (d, J_{RhH} = 11.0 Hz, overlapping with toluene- d_8, *CH*$_2$), 2.83 (d, J_{RhH} = 11.0 Hz, 2H, *CH*$_2$), 5.98 (t, J_{HH} = 6.3 Hz, 1H, *CH*$_2$), 6.35 (s, 1H), 6.45 (t, J_{HH} = 7.8 Hz, 1H), 6.78 (d, J_{HH} = 5.0 Hz, 1H), 6.95−7.25 (m, overlapping with toluene-d_8), 7.46 (d, J_{HH} = 10.0 Hz, 2H), 7.62 (d, J_{HH} = 11.0 Hz, 2H). ^1H NMR (−60 °C, toluene-d_8, 500 MHz): δ 2.05 (d, J_{HH} = 11.5 Hz, 2H), 2.09 (overlaps with toluene-d_8), 2.75 (d, J_{HH} = 11.5 Hz, 2H), 4.08 (J_{HH} = 14.0 Hz, 2H), 5.88 (t, J_{HH} = 6.3 Hz, 1H), 6.36 (t, J_{HH} = 7.75 Hz, 1H), 6.48 (s, 1H), 6.63 (d, J_{HH} = 5.0 Hz, 1H), 7.05−7.45 (m, overlapping with toluene-d_8), 7.54 (d, J_{HH} = 10.0 Hz, 2H), 7.72 (d, J_{HH} = 10.0 Hz, 2H). $^{13}C\{^1H\}$ NMR (C_6D_6, 125.7 MHz): δ 60.8 (d, J_{RhC} = 12.1 Hz,), 64.8 (d, J_{RhC} = 12.1 Hz), 116.94, 117.55, 118.92, 126.63, 127.09, 127.91, 128.56, 128.76, 129.75, 129.94, 130.51, 137.13, 138.11, 139.0, 142.58, 147.92, 159.31. Anal. Calcd for $C_{25}H_{23}N_2Rh$: C, 66.08; H, 5.10; N, 6.17. Found: C, 65.87; H, 5.02; N, 5.89.

Alternative Synthesis of (PyPyr)Rh(C_2H_4)$_2$ (3). Solid $LiN(SiMe_3)_2$ (0.080 mg, 0.48 mmol) was added to a stirred, room-temperature solution of **2** (0.020 g, 4.1 mmol) in 5 mL of benzene. The reaction mixture was allowed to stir at ambient temperature for 12 h, after which it was filtered. Volatile materials were removed under vacuum, and the resulting solids were washed with pentane (2 × 1.5 mL). The precipitate was evacuated to dryness to afford **3** as an analytically pure brown solid (0.120 g, 64%). The acquired ^1H NMR (benzene-d_6) spectrum was identical to that of samples obtained by the synthesis given above. Anal. Calcd for $C_{25}H_{23}N_2Rh$: C, 66.08; H, 5.10; N, 6.17. Found: C, 65.81; H, 5.23; N, 6.08.

(PyPyr)Rh(COD) (4). A 3 mL benzene slurry of **1** (0.054 g, 0.888 mmol) was added to a stirred, room-temperature solution of $[RhCl(COD)]_2$ (0.805 g, 2.08 mmol) in 0.5 mL of benzene. The reaction mixture was allowed to stir at ambient temperature for 4 h, and was then filtered. The solution was concentrated to 0.5 mL under vacuum, and product was then precipitated with hexane. The supernatant was removed and the solid was dried in vacuo to afford **4** as an analytically pure brown solid (0.0462 g, 50.7%). ^1H NMR (C_6D_6, 500 MHz): δ 1.49 (m, 4 H, *CH*$_2$), 2.10 (m, 4 H, *CH*$_2$), 3.63 (br s, 2 H, *CH*), 4.73 (br s, 2 H, *CH*$_2$), 5.90 (t, $^3J_{HH}$ = 5.8 Hz, 1H), 6.49 (overlapping multiplet, 2 H), 6.88 (d, 1 H, $^3J_{HH}$ = 4.8 Hz), 7.06−7.28 (m, overlapping with benzene-d_6), 7.56 (d, 2 H, $^3J_{HH}$ = 7.56 Hz), 7.72 (d, 2 H, $^3J_{HH}$ = 6.8 Hz). $^{13}C\{^1H\}$ NMR (C_6D_6, 121.7 MHz): δ 30.26. 30.91, 77.65 (d, J_{RhC} = 13.1 Hz), 80.39 (d, J_{RhC} = 12.07 Hz), 116.82, 117.26, 119.08, 127.14, 127.96, 128.72, 129.63, 129.88, 129.96, 130.52, 136.95, 137.28, 139.08, 139.30, 145.09, 148.69 (d, J_{RhC} = 2.0 Hz), 159.53. Anal. Calcd for $C_{29}H_{27}N_2Rh$: C, 68.78; H, 5.37; N, 5.53. Found: C, 68.83; H, 5.27; N, 5.70.

(71) Connolly, J. W.; Urry, G. *Inorg. Chem.* **1963**, *2*, 645–646.

(PyPyr)Ir(COD) (5). A 3 mL benzene slurry of **1** (0.060 g, 0.198 mmol) was added to a stirred, room-temperature solution of $[IrCl(COD)]_2$ (0.067 g, 2.08 mmol) in 0.5 mL of benzene. The reaction mixture was allowed to stir at ambient temperature for 16 h, and then it was filtered. The solution was concentrated under vacuum, and product was then crystallized by vapor diffusion of pentane into the benzene solution at 25 °C. Three crops of crystals were collected and dried under vacuum to afford **5** as an analytically pure orange solid (0.040 g, 34%). ^{1}H NMR (C_6D_6, 500 MHz): δ 1.49 (m, 4 H, *CH*$_2$), 2.10 (m, 4 H, *CH*$_2$), 3.39 (m, 2 H, *CH*), 4.60 (m, 2 H, *CH*), 5.87 (t, 1 H, $^3J_{HH}$ = 6.2 Hz), 6.39 (s, 1 H), 6.45 (t, 1 H, $^3J_{HH}$ = 7.6 Hz), 7.08−7.25 (m, overlapping with benzene-d_6), 7.29 (d, 1 H, $^3J_{HH}$ = 8.4 Hz), 7.51 (d, 2 H, $^3J_{HH}$ = 5.1 Hz), 7.92 (d, 2 H, $^3J_{HH}$ = 7.2 Hz). ^{13}C{^{1}H} NMR (C_6D_6, 121.7 MHz): δ 30.95, 32.22, 60.75, 65.13, 117.83, 118.05, 118.66, 126.81, 127.56, 128.32, 128.77, 129.92, 130.22, 131.24, 137.58, 138.36, 138.42, 139.18, 144.99, 149.16, 160.00. Anal. Calcd for $C_{29}H_{27}N_2Ir$: C, 58.47; H, 4.57; N, 4.70. Found: C, 58.28; H, 4.79; N, 4.58.

(PyPyr)Rh(CO)$_2$ (6). A 2 mL benzene slurry of **1** (0.0385 g, 0.127 mmol) was added to a stirred solution of $[RhCl(CO)_2]_2$ (0.0247 g, 0.0635 mmol) in 2 mL of benzene. The reaction mixture was allowed to stir at ambient temperature for 18 h, and then it was filtered. The solution was concentrated under vacuum, and the product was crystallized by vapor diffusion of hexane into the benzene solution at 25 °C. Red crystals were collected and dried under vacuum to afford **6** as red solid (0.0096 mg, 17%). ^{1}H NMR (C_6D_6, 500 MHz): δ 5.78 (t, $^3J_{HH}$ = 6.4 Hz, 1H), 6.42 (t, $^3J_{HH}$ = 7.8 Hz, 1H), 6.54 (s, 1H), 7.10−7.35 (m, overlapping with benezene-d_6), 7.51 (d, $^3J_{HH}$ = 7.6 Hz, 2H), 7.63 (d, $^3J_{HH}$ = 5.6 Hz, 1H), 7.72 (d, $^3J_{HH}$ = 7.6 Hz, 2H). IR (cm^{-1}): 2004 (CO), 2067 (CO).

Alternative Synthesis of (PyPyr)Rh(CO)$_2$ (6). Carbon monoxide (1 atm) was bubbled through a stirred solution of **3** (0.261 g, 0.479 mmol) in 30 mL of benzene for 1 h. The volatile material was removed to afford **6** as an analytically pure orange solid (0.261 g, 99%). The ^{1}H NMR spectrum is identical to that of the prior synthesis. ^{13}C{^{1}H} NMR (C_6D_6, 121.7 MHz): δ 114.65, 117.88, 118.94, 127.02, 127.62, 128.85, 129.82, 129.68, 130.33, 132.34, 136.43, 137.89, 138.28, 138.83, 149.15 (d, J_{RhC} = 3.0 Hz), 151.49, 158.95, 184.94 (d, J_{RhC} = 70.3 Hz), 187.88 (d, J_{RhC} = 64.4 Hz). Anal. Calcd for $C_{23}H_{15}N_2O_2Rh$: C, 60.81; H, 3.33; N, 6.17. Found: C, 60.93; H, 3.58; N, 5.82.

(PyPyr)Ir(CO)$_2$ (7). A 3 mL benzene slurry of **1** (0.0490 g, 0.162 mmol) was added to a stirred solution of $IrCl(CO)_3$ (0.0670 g, 2.08 mmol) in 0.5 mL of benzene. The reaction mixture was allowed to stir at 25 °C for 26 h. The mixture was then filtered and concentrated under vacuum. Vapor diffusion of hexane into the solution of the product at 25 °C yielded red crystals of **7** (0.0085 g, 9.7%). ^{1}H NMR (C_6D_6, 500 MHz): δ 5.68 (t, $^3J_{HH}$ = 6.2 Hz, 1H), 6.35 (t, $^3J_{HH}$ = 7.4 Hz, 1H), 6.46 (s, 1H), 7.12−7.26 (m, overlapping with benzene-d_6), 7.45 (d, $^3J_{HH}$ = 7.2 Hz, 2H), 7.71 (d, $^3J_{HH}$ = 7.2 Hz, 2H), 7.83 (d, $^3J_{HH}$ = 5.6 Hz, 1H). ^{13}C{^{1}H} NMR (C_6D_6, 121.7 MHz): δ 115.39, 118.68, 118.79, 127.34, 128.31, 128.79, 128.89, 129.75, 130.75, 133.23, 137.40, 137.51, 137.74, 138.40, 149.95, 151.37, 158.66, 172.61, 178.87. Anal. Calcd for $C_{23}H_{15}N_2IrO_2$: C, 50.82; H, 2.78; N, 5.15. Found: C, 50.61; H, 2.83; N, 5.24. IR (cm^{-1}): 1986 (CO), 2050 (CO).

(PyPyr)Rh(H)$_2$(SiEt$_3$)$_2$ (8). Neat $HSiEt_3$ (0.0215 g, 0.185 mmol) was added to a solution of **3** (0.0180 g, 0.0396 mmol) in 0.5 mL of benzene. The reaction mixture was allowed to stir at ambient temperature for 0.5 h, and the volatile materials were then removed under vacuum. The resulting solid was washed with hexane (5 × 3 mL) and dried in vacuo to afford **8** as an analytically pure red-brown solid (0.0126 g, 50.4%). ^{1}H NMR (C_6D_6, 500 MHz): δ −15.43 (dd, 1 H, J_{RhH} = 25.5 Hz, J_{HH} = 9.5 Hz, Rh*H*), −14.64 (dd, 1 H, J_{RhH} = 25.0 Hz, J_{HH} = 9.5 Hz, Rh*H*), 0.54 (t, 18 H, *CH*$_3$), 0.97 (q, 12 H, *CH*$_2$), 6.12 (t, 1 H, $^3J_{HH}$ = 5.2 Hz), 6.56 (t, 1 H, $^3J_{HH}$ = 7.2 Hz), 6.63 (s, 1 H), 7.12−7.26 (m, overlapping with benzene-d_6), 7.36 (m, 4 H), 7.63 (d, 2 H, $^3J_{HH}$ = 5.2 Hz), 8.00 (d, 2 H, $^3J_{HH}$ = 3.6 Hz), 8.18 (d, 1 H, $^3J_{HH}$ = 4.4 Hz). ^{13}C{^{1}H} NMR (C_6D_6, 121.7 MHz): δ 8.41, 12.26, 115.29, 118.03, 119.10, 126.43, 126.75, 127.94, 128.72, 129.65, 130.02, 132.21, 137.48, 137.97, 139.15, 139.46, 147.67 (d, J_{RhC} = 4.6 Hz), 151.8, 158.46. ^{29}Si NMR (via ^{1}H,^{29}Si gHMBC, C_6D_6, 99.3 MHz): δ 78.8 (J_{RhSi} = 25.3, J_{SiH} = 11.6 Hz, J_{SiH}' = 4.8 Hz). Anal. Calcd for $C_{33}H_{47}N_2RhSi_2$: C, 62.83; H, 7.51; N, 4.44. Found: C, 63.17; H, 7.22; N, 4.48.

(PyPyr)Rh(H)$_2$(SiPh$_3$)$_2$ (9). A 2 mL solution of $HSiPh_3$ (0.0916 g, 0.352 mmol) was added to a solution of **3** (0.0400 g, 0.0880 mmol) in 3 mL of benzene. The reaction mixture was stirred at 25 °C for 0.5 h, and then the volatile materials were removed under vacuum. The resulting solid was dissolved into a minimum volume of diethyl ether, then precipitated with 3 mL of pentane at −30 °C. Precipitation was repeated three times, and the resulting solid was dried under vacuum to afford **9** as an analytically pure red solid (0.0621 g, 76.8%). ^{1}H NMR (C_6D_6, 500 MHz): δ −13.20 (dd, 1 H, J_{RhH} = 22.0 Hz, J_{HH} = 8.0 Hz, Rh*H*), −11.90 (dd, 1 H, J_{RhH} = 23.0 Hz, J_{HH} = 8.0 Hz, Rh*H*), 5.77 (t, 1 H, $^3J_{HH}$ = 6.4 Hz), 6.31 (s, 1 H), 6.45 (t, 1 H, $^3J_{HH}$ = 8.4 Hz), 7.06 (m, 18 H), 7.12−7.26 (m, overlapping with benzene-d_6), 7.43 (d, 2 H, $^3J_{HH}$ = 7.2 Hz), 7.58 (m, 14 H). ^{13}C{^{1}H} NMR (C_6D_6, 121.7 MHz): δ 115.33, 117.68, 118.81, 126.56, 127.07, 128.54, 129.60, 129.64, 129.70, 129.81, 129.89, 130.66, 136.77, 137.14, 137.81, 138.05, 139.08, 139.64, 147.67 (d, J_{RhC} = 2.6 Hz), 151.80, 158.46. ^{29}Si NMR (via ^{1}H,^{29}Si gHMBC, C_6D_6, 99.3 MHz): δ 49.1 (J_{RhSi} = 22.4 Hz, J_{SiH} = 19.4 Hz, J_{SiH}' = 7.4 Hz). Anal. Calcd for $C_{57}H_{47}N_2RhSi_2$: C, 74.49; H, 5.15; N, 3.05. Found: C, 74.40; H, 5.18; N, 2.95.

(PyPyr)Rh(H)$_2$(SiPh$_2$^{t}Bu)$_2$ (10). Neat HSi^tBuPh_2 (0.0850 g, 0.354 mmol) in benzene was added to a stirred, room-temperature solution of **3** (0.0400 g, 0.088 mmol) in 3 mL of benzene. The reaction mixture was stirred at 25 °C for 0.5 h, and the volatile materials were removed under vacuum. The resulting solid was dissolved into a minimum volume of diethyl ether, and then precipitated with 3 mL pentane at −30 °C. Precipitation was repeated as above three times, and the resulting solid was dried under vacuum to afford **10** as an analytically pure red solid (0.0516 mg, 66.7%). ^{1}H NMR (C_6D_6, 500 MHz): δ −14.64 (dd, 1 H, J_{RhH} = 19.2 Hz, J_{HH} = 9.6 Hz, Rh*H*), −13.02 (dd, 1 H, J_{RhH} = 24.4 Hz, J_{HH} = 9.6 Hz, Rh*H*), 1.00 (s, 18 H, C*CH*$_3$), 5.85 (t, 1 H, $^3J_{HH}$ = 6.0 Hz), 6.38 (s, 1 H), 6.54 (t, 1 H, $^3J_{HH}$ = 7.6 Hz), 7.05−7.46 (m, overlapping with benzene-d_6), 7.53 (d, 2 H, $^3J_{HH}$ = 8.0 Hz), 7.61 (m, 1H), 7.68 (m, 4 H), 7.75 (d, 2 H, $^3J_{HH}$ = 3.2 Hz). ^{13}C{^{1}H} NMR (C_6D_6, 121.7 MHz): δ 24.4, 29.01, 115.88, 117.64, 118.79, 126.57, 127.27, 127.64, 127.86, 128.67, 129.78, 129.98, 130.51, 136.09, 136.32, 136.77, 137.79, 138.09, 139.38, 139.77, 146.89 (d, J_{RhC} = 2.6 Hz), 151.24, 157.97. ^{29}Si NMR (via ^{1}H,^{29}Si gHMBC, C_6D_6, 99.3 MHz): δ 56.6 (J_{RhSi} = 21.8 Hz, J_{SiH} < 0.2 Hz). Anal. Calcd for $C_{53}H_{55}N_2RhSi_2$: C, 72.41; H, 6.31; N, 3.19. Found: C, 72.21; H, 6.55; N, 3.20.

(PyPyr)Ir(H)$_2$(SiPh$_3$)$_2$ (11). A 2 mL benzene solution of **1** (0.0661 g, 0.223 mmol) was added to a stirred, room-temperature suspension of $[ClIr(COE)_2]_2$ (0.1000 g, 0.112 mmol) in 2 mL of benzene. After stirring for 15 min, solid $HSiPh_3$ (0.179 g, 0.687 mmol) was added in portions. After stirring for 0.5 h the reaction mixture was filtered, and the resulting solution was concentrated under vacuum. A solid was precipitated upon addition of 2 mL of pentane. The supernatant was removed, and the solid was dissolved in 2 mL of benzene, and precipitation with pentane was repeated three times. The resulting solid was dried under vacuum to afford **11** as an analytically pure red powder (0.149 g, 66.3%). ^{1}H NMR (C_6D_6, 500 MHz): δ −15.80 (d, 1 H, $^2J_{HH}$ = 2.7 Hz, Ir*H*), −13.98 (d, 1 H, $^2J_{HH}$ = 2.7 Hz, Ir*H*), 5.65 (t, 1 H, $^3J_{HH}$ = 6.5 Hz), 6.24 (s, 1 H), 6.40 (t, 1 H, $^3J_{HH}$ = 7.8 Hz), 7.05 (m,18 H,), 7.19−7.30 (m, 8 H), 7.39 (d, 1 H, $^3J_{HH}$ = 7.5 Hz), 7.54 (d, 12 H, $^3J_{HH}$ = 7.0 Hz), 7.72 (d, $^3J_{HH}$ = 5.0 Hz, 2 H). ^{13}C{^{1}H} NMR (C_6D_6, 121.7 MHz): δ 116.22, 118.64, 118.91, 126.81, 127.04, 128.35, 128.59, 128.70, 129.37, 129.72, 130.59, 135.85, 136.59, 137.35, 138.04, 138.84, 139.11, 140.21, 149.35, 152.87, 158.57.^{29}Si NMR (via ^{1}H,^{29}Si gHMBC, C_6D_6, 99.3 MHz): δ 8.3 (J_{SiH} = 1.9 Hz, J_{SiH}' = 1.9 Hz).

Anal. Calcd for $C_{57}H_{47}N_2IrSi_2$: C, 67.89; H, 4.70; N, 2.78. Found: C, 68.07; H, 4.90; N, 3.11.

(PyPyr)Rh(μ-H)$_2$(μ-Si^{t}Bu$_2$)Rh(PyPyr) (12). A 2 mL solution of $H_2Si^tBu_2$ (0.0126 g, 0.088 mmol) was added to a solution of **3** (0.0400 g, 0.088 mmol) in 3 mL of benzene. The reaction mixture was stirred at 25 °C for 2 h, and then the volatile materials were removed under vacuum. The resulting solid was washed with 3 mL of diethyl ether, and then dissolved into a minimum amount of benzene. Addition of diethyl ether at 25 °C precipitated red-orange analytically pure crystals of **12** (0.0267 g, 32.2%). ^{1}H NMR (benezene-d_6): δ −24.25 (t, 2 H, J_{RhH} = 32.4, T1 = 0.583 s, Rh*H*), 0.76 (s, 18 H, C*CH*$_3$), 5.81 (d, 2 H, $^3J_{HH}$ = 5.6 Hz), 6.63 (s, 2 H), 7.12−7.26 (m, overlapping with benzene-d_6), 7.30−7.45 (overlapping m), 7.16 (d, 4 H, $^3J_{HH}$ = 7.2 Hz), 7.98 (d, 2 H, $^3J_{HH}$ = 6.0 Hz). ^{13}C{^{1}H} NMR (benzene-d_6): δ 22.52, 105.48, 108.29, 109.29, 117.76, 118.74(d, J_{RhC} = 7.5 Hz), 120.59, 120.81, 121.91, 122.12, 124.43, 128.65, 129.10, 129.94, 130.31, 130.68, 140.36, 147.09, 150.79. ^{29}Si NMR (via ^{1}H,^{29}Si gHMBC): δ 252.84. Anal. Calcd for $C_{50}H_{50}N_4Rh_2Si$: C, 63.83; H, 5.36; N, 5.95. Found: C, 63.49; H, 5.58; N, 5.71.

[(PyPyr)Rh(μ-H)(Si^{t}BuPh$_2$)]$_2$ (13). Neat HSi^tBuPh_2 (0.1120 g, 0.465 mmol) was added to a stirred, room-temperature solution of **3** (0.0500 g, 0.111 mmol) in 3 mL of benzene. The temperature of the reaction mixture was elevated to 75 °C for 9 h. The volatile material was then removed under vacuum. The resulting solid was dissolved into a minimum volume of methylene chloride, and vapor diffusion of 3 mL ether into the methylene chloride solution at −30 °C gave **13** as brown plates (0.0304 g, 66.7%). ^{1}H NMR (C_6D_6, 500 MHz): δ −21.99 (t, 2 H, $^1J_{RhH}$ = 33.6 Hz, Rh*H*), 0.56 (s, 18 H, C*CH*$_3$), 5.90 (t, 2 H, $^3J_{HH}$ = Hz), 6.49 (t, 2 H, $^3J_{HH}$ = Hz), 6.54 (s, 2 H), 6.82 (m, 2H), 6.95 (br m, 2H), 7.05 (m, 4H), 7.10−7.30 (m, overlapping with benzene-d_6), 7.37 (m, 4H), 7.59 (d, 4 H, $^3J_{HH}$ = 7.6 Hz), 7.77 (br m, 4 H), 8.10 (d, 4 H,$^3J_{HH}$ = 6.4 Hz). ^{29}Si NMR (via ^{1}H,^{29}Si gHMBC, C_6D_6, 99.3 MHz): δ 33.1. ^{13}C{^{1}H} NMR (C_6D_6, 121.7 MHz): δ 27.7, 115.6, 116.2, 117.2, 125.4, 126.5, 127.2, 128.1, 128.6, 129.4, 130.8, 132.5, 134.7, 135.2, 135.7, 136.5, 137.0, 137.7, 138.4, 138.7, 148.2, 155.5, 156.6.

(PyPyr)RhH(SiPh$_3$)(PPh$_3$) (14). A 2 mL solution of $HSiPh_3$ (0.110 g, 0.440 mmol) was added to a stirred, room-temperature solution of **3** (0.0400 g, 0.0880 mmol) in 3 mL of benzene. To the mixture, PPh_3 (0.115 g, 0.440 mmol) of was added. The reaction mixture was stirred at ambient temperature for 2 h, and then the volatile material was removed under vacuum. The resulting solid was dissolved into a minimum volume of benzene, then precipitated with 3 mL hexane at 25 °C. Red crystals of **14** were isolated (0.0811 g, 72.5%). ^{1}H NMR (C_6D_6, 500 MHz): δ −12.94 (dd, 1 H, J_{RhH} = 28.8 Hz, J_{PH} = 20.4 Hz, Rh*H*), 6.15 (t, 1 H, $^3J_{HH}$ = 6.8 Hz), 6.54 (s, 1 H), 6.74 (t, 1 H, $^3J_{HH}$ = 7.2 Hz), 7.12−7.26 (m, overlapping with benzene-d_6), 7.42 (m, 6 H), 7.50−7.61 (m, 10 H). ^{31}P NMR (C_6D_6, 161.9 MHz): δ 42.27 (q, J_{RhP} = 138.0 Hz, J_{PH} = 20.4 Hz). ^{13}C{^{1}H} NMR (C_6D_6, 121.7 MHz): δ 116.49, 118.60, 125.8 (d, J_{PC} = 36.4 Hz), 126.68, 126.98, 127.27, 127.53, 127.73, 128.05, 128.15, 128.32 (d, J_{RhC} = 8.8 Hz), 129.62, 129.94, 130.72, 132.35 (d, J_{PC} = 44.0 Hz), 132.53, 133.48 (d, J_{RhC} = 10.1 Hz), 136.21, 136.67, 141.42, 150.13. ^{29}Si NMR (via ^{1}H,^{29}Si gHMBC, C_6D_6, 99.3 MHz): δ 32.2 (J_{SiRh} = 37.7 Hz, J_{SiP} = 9.9 Hz). Anal. Calcd for $C_{57}H_{46}N_2RhPSi$: C, 74.34; H, 5.03; N, 3.04. Found: C, 74.67; H, 5.39; N, 2.66.

General Procedure for Catalytic Runs. Reactions were conducted in 5 mm Wilmad NMR tubes equipped with a J. Young Teflon-valve seal, which were heated in temperature-controlled oil baths. Samples were prepared in the drybox by dissolving 5 mol % catalyst, silane (1 equiv), and olefin or alkyne (1 equiv) in 1 mL of C_6D_6. Reaction progress was monitored by ^{1}H NMR spectroscopy. Product compositions were confirmed by GCMS.

Kinetic Measurements. Reactions were monitored by ^{1}H NMR spectroscopy, on a Bruker DRX-500 spectrometer, using 5 mm Wilmad NMR tubes fitted with septa. The samples were prepared by dissolution of **10** in 1 mL of C_6D_6 that was then cooled to −78 °C followed by addition of the $HSiEt_3$ via a syringe. The NMR tube was quickly placed in the probe, which was precooled or preheated to the required temperature. The probe temperature was calibrated using a neat methanol sample prior to the experiment and was monitored throughout the experiment with a thermocouple. Single-scan spectra were obtained using an automated acquisition program that was started immediately after placing the sample in the probe, and the peaks were integrated relative to the intensity of a known concentration of ferrocene standard. Rate constants were obtained by nonweighted linear least-squares fit of the integrated first-order rate law. The rate law determination was performed at 323 K in C_6D_6. For the Eyring analysis, measurements were performed in toluene-d_8 between 236.2 and 275.8 K.

X-ray Structure Determinations. The X-ray analyses of compounds **4**, **5**, **9**, **10**, **11**, **12**, **13**, and **14** were carried out at UC Berkeley CHEXRAY crystallographic facility. Measurements were made on Bruker SMART CCD area detector with graphite-monochromated Mo Kα radiation (λ = 0.71073 Å). Data were integrated by the program SAINT and analyzed for agreement using XPREP. Empirical absorption corrections were made using SADABS. Structures were solved by direct methods and expanded using Fourier techniques. All calculations were performed using the SHELXTL crystallographic package. All non-hydrogen atoms were refined anisotropically unless otherwise stated and hydrogen atoms were placed in their calculated positions.

For **4**: Crystals were grown from vapor diffusion of pentane into benzene at 25 °C.

For **5**: Crystals were grown from vapor diffusion of pentane into benzene at 25 °C.

For **9**: Crystals were grown from vapor diffusion of pentane into THF at −30 °C.

For **10**: Crystals were grown from vapor diffusion of pentane into THF at −30 °C.

For **11**: Crystals were grown from vapor diffusion of pentane into THF at −30 °C.

For **12**: Crystals were grown from vapor diffusion of diethyl ether into benzene at 25 °C.

For **13**: Crystals were grown from vapor diffusion of diethyl ether into methylene chloride at −30 °C.

For **14**: Crystals were grown from vapor diffusion of diethyl ether into benzene at 25 °C.

Acknowledgment. Acknowledgement is made to Dr. Herman van Halbeek for assistance with Si/H NMR experiments, and to Dr. Fred Hollander and Dr. Allen Oliver for assistance with the X-ray crystallography. This work was supported by the Director, Office of Energy Research, Office of Basic Energy Sciences, Chemical Sciences Division of U.S. Department of Energy under Contract No. DE-AC02-05CH11231.

Supporting Information Available: Kinetic data and X-ray experimental details and crystallographic data for **4**, **5**, **9**, **10**, **11**, **12**, **13**, and **14**. This material is available free of charge via the Internet at http://pubs.acs.org.

JA9035169